Advances in the controlled growth of nanoclusters using a dendritic architecture†

Jason K. Vohs[a] **and Bradley D. Fahlman***[b]

Received (in Montpellier, France) 10th November 2006, Accepted 6th February 2007
First published as an Advance Article on the web 7th March 2007
DOI: 10.1039/b616472m

The dendritic architecture represents the fourth major class of polymers. Though hyperbranched polymers and structurally-perfect dendrimers (*e.g.*, poly(amidoamine), PAMAM) both share this designation, the latter are of greater use for nanoreactor applications. One such application that exploits the container/reactor properties of dendrimers is the controlled growth of nanoclusters. Herein, we provide a review of the recent synthetic methods for nanocluster growth using a dendritic host, and their use in a variety of applications. The benefits of using this macromolecular host will also be discussed, within a historical context of colloidal entraining agents.

1 Historical background

There is much current interest in the synthesis of 0-D nanostructures for next-generation (opto)electronics,[1] sensors,[2] catalysts,[3] battery electrolytes,[4] multifunctional coatings,[5] and biomedical applications.[6] However, the use of these nanomaterials actually dates back to at least to the 16th century from the colloidal gold potions (*aurum potabile*) reported by Paracelsus.[7] The first materials-related application for nanoparticles was colored glass, pioneered by Cassius and Kunchel in the 17th century.[8] However, it should be noted that these early applications employed nanoparticles with an extremely large polydispersity—most likely consisting of both nanosized and sub-micron species. Faraday's work in the mid-19th century represents the first chemical route toward nanoparticulate metals, through phosphorus reduction of gold chloride solutions. This pioneering work was also the first to determine the influence of particle size on the resultant color, preceding the more detailed work of Raleigh.[7] However, it was not possible to control the diameters of the nanostructures using these early synthetic techniques.

The typical route for solution-phase growth of metal nanoparticles/nanoclusters is the simple reduction of metal salts, usually *via* $NaBH_4$, H_2 or hydrazine as reducing agents (for example, eqn (1)).[9] In theory, any metal with a larger standard reduction potential (E°) than the reducing agent (*e.g.*, -0.481 V for borohydride ion) is a candidate for reduction to its metallic form. This includes most of the first-row transition metal ions, and many others from the main group/transition metal series. However, it should be noted that solution pH and side-reactions (*e.g.*, metal ions being converted to borides by

Jason K. Vohs was born in Charleston, SC in 1977. He attended the College of Charleston, where he received his BS/AB (cum laude 1999) degrees in chemistry, biochemistry, and classical studies. He received his PhD (with Gregory H. Robinson) from the University of Georgia (2003) working on the preparation of main group metal complexes utilizing sterically hindering ligands. He was a postdoctoral researcher with Bradley D. Fahlman (2003–2005) working on nanostructural thin films and materials. He is currently an assistant professor of chemistry at Saint Vincent College.

Bradley D. Fahlman was born in Regina, Saskatchewan, Canada in 1972. He received his BSc in Chemistry (High Hons.) from the University of Regina in 1996, and his PhD in Inorganic Chemistry (with Andrew R. Barron) from Rice University in 2000. After serving as the Director of Advanced Laboratories and Lecturer in Chemistry at the University of California, Irvine (2000–2002), Dr Fahlman joined the faculty at Central Michigan University, receiving early tenure and promotion to Associate Professor in 2005. His current research interests include low-temperature nanostructural growth and chemical vapor deposition of high-k dielectric thin films, including novel precursor design.

---

[a] *Department of Chemistry, St. Vincent College, Latrobe, PA 15650, USA*
[b] *Department of Chemistry, Central Michigan University, Mount Pleasant, MI 48859, USA*

† This paper was published as part of the special issue on Dendrimers and Dendritic Polymers: Design, Properties and Applications.

BH_4^- rather than reduction) often provide a barrier toward successful metal ion reduction.

$$Cu^{2+} + 2\,Cl^- + 6\,H_2O + 2\,NaBH_4 \rightarrow Cu^0 + 2\,NaCl + 7\,H_2 + 2\,B(OH)_3 \quad (1)$$

If the above reaction is carried out in solution as-is, a bulk metal powder (and metallic film along the flask sidewalls) will preferentially form. Early synthetic methods likely employed additives (*e.g.*, organic matter, clays, *etc.*) that serendipitously prevented agglomeration allowing for some degree of nanoparticulate growth. However, it wasn't until the mid 1950s that stabilizing agents were purposefully used to prevent aggregation of the growing nanostructures. Most of the early work employed polydispersed organic polymers and ionic species to stabilize colloidal suspensions (*e.g.*, the Turkevich process using sodium citrate (**I**),[10] or the use of bis(11-trimethylammoniumdecanoylaminoethyl)disulfide dibromide (TADDD, **II**)[11]—a recent extension of the Brust method[12]). The use of ates serves a two-fold purpose: as both an entrainer species and the reducing agent for metal nanostructural growth.

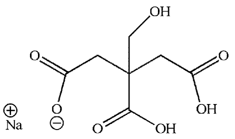

I

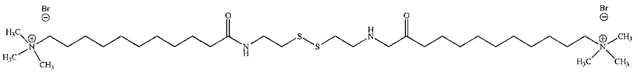

II

The use of polyoxoanion stabilizers for Ir nanocluster growth by Finke *et al.* in 1990 represented an important precedent for 0-D nanostructural growth. This work represented the first time that nanoclusters could be synthesized with strict control over resultant diameters and catalytic properties—not previously possible for traditional colloids (Table 1).[13] In addition, this system has also been used to decipher the four-step mechanism for nanocluster growth;[14] perhaps even more useful for the continued development of nanocluster-based applications.

A wide variety of other species have been used to control 0-D nanostructural growth. For example, Schaak *et al.* have recently utilized polymers such as poly(vinylpyrrolidone) (PVP, **III**), poly(styrenesulfonic acid) sodium salt (PSS, **IV**), and poly(2-ethyl-2-oxazoline) (PEO, **V**) to afford nanoparticle growth, including nanoalloy formation at temperatures of *ca.* 200 °C, aptly referred to as "metallurgy in a beaker".[16] The PVP architecture has also been shown to facilitate the growth of Au@Ag core–shell nanostructures,[17] as well as Ag nanowires and nanocubes.[18]

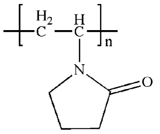

III

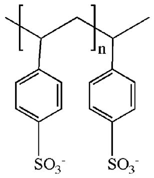

IV

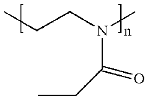

V

It is not always necessary for the metal ions to be initially encapsulated within a stabilizing polymer prior to reduction. For instance, there are precedents for a post-reduction living radical polymerization that takes place on the surface of gold nanoparticles.[19] This results in a dense "polymer brush" that encapsulates the metallic nanoparticle, effectively stabilizing the structure against agglomeration. Subsequent alignment and surface reactivity of the resultant nanostructures may be fine-tuned by varying the nature of the polymer coating.

2 Dendrimer-encapsulated nanoclusters: synthetic strategies

In order to afford monodisperse nanoclusters of a form most useful for applications, a stabilizing (or entraining) agent should be:[20]

(i) Chemically unreactive toward the growing nanocluster, rendering an unpassivated nanocluster surface;

(ii) Structurally well-defined (size/shape), which allows for the controlled growth of the encapsulated nanocluster;

(iii) Comprised of light elements (organic-based), so its structure doesn't interfere with the characterization of the entrained nanocluster. This will also facilitate its sacrificial removal from the nanocluster by pyrolysis at relatively low temperatures, if desired;

(iv) Surface-modifiable, to allow for tunable solubility and selective interactions with external stimuli. In addition, to afford controllable self-assembly of entrained nanoclusters on a variety of surfaces through chemisorption, if desired.

All of these above requirements are made possible through use of dendritic architectures. Not only is one able to control the diameter of the resultant nanocluster through structural variations (core and periphery), but its solubility and surface reactivity may also be fine-tuned through varying of the

Table 1 Comparison of 0-D nanostructures with traditional colloids[15]

Nanoparticles/nanoclusters	Colloids
Size: 1–100 nm (nanoclusters: 1–10 nm)	Typically >10 nm
Homogeneous molecular composition	Poorly defined compositions
≤15% size dispersion (less polydispersity for nanoclusters relative to nanoparticles)	>15% size dispersion
Reproducible synthesis (control over size, shape, and composition)	Non-reproducible, uncontrollable morphology/composition
Reducible physical properties and catalytic activity	Non-reproducible properties (esp. irreproducible catalytic activities)
Soluble in polar/non-polar organic solvents (depending on stabilizing agent)	Typically only soluble in polar solvents
Contain clean surfaces	Contain surface-adsorbed species such as –OH, –X, $-OH_2$, *etc.*

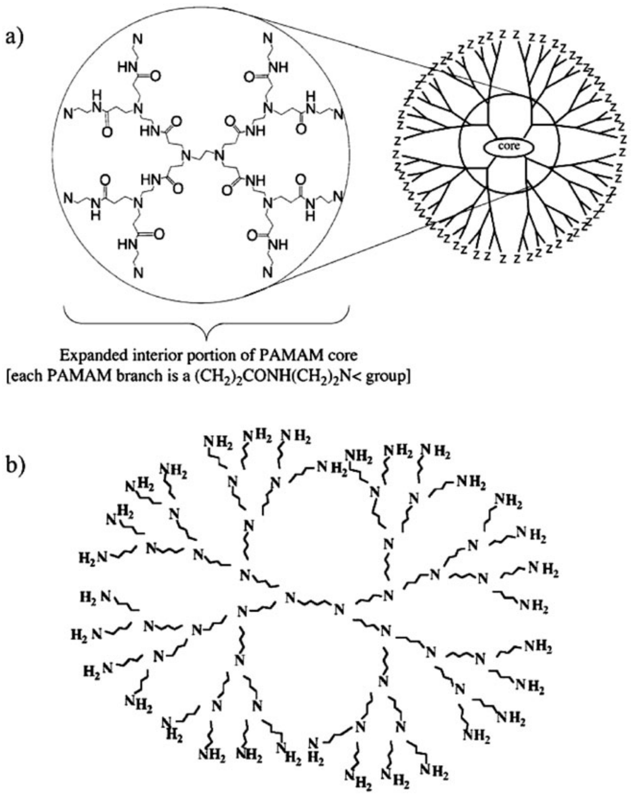

Fig. 1 Molecular structures of (a) G5-PAMAM and (b) G4-PPI amine-terminated dendrimers.[29]

peripheral groups. The structurally-perfect poly(amidoamine) (PAMAM, Fig. 1(a)) dendritic architecture was first applied to entrain Cu nanoclusters in 1998, as reported by Crooks[21] and then shortly afterwards by Tomalia and co-workers.[22] Three years later, the poly(propyleneimine) dendrimer (PPI, Fig. 1(b)) was first used by Crooks *et al.* for Cu^0 nanocluster growth.[23]

In general, as the number of branching units (generation #, G) increases from the core, so does its surface density, which prevents the incoming metal ion from entering the interior of the dendritic architecture. Alternatively, for smaller generations, the entrained species becomes easily dislodged from the interior due to its open structure. Hence, the most effective PAMAM size range for nanocluster growth is between the fourth and sixth generations (G4–G6), which exhibit strong container properties (Fig. 2). It should be noted that for equivalent generations, the diameter of PPI dendrimers are smaller than PAMAM (*e.g.*, for G4—2.8 nm and 4.5 nm for PPI and PAMAM, respectively), which affects the sizes of the corresponding inter- and intradendrimer-stabilized nanoclusters. In addition, the PPI dendrimer is more thermally robust than PAMAM. Whereas temperatures >250 °C are required to decompose PPI, the PAMAM dendrimer begins to lose amide linkages at temperatures as low as 75 °C, with complete decomposition accomplished at 300 °C.[24]

The earliest examples of M@dendrimer nanocluster growth featured the use of amine-terminated dendrimers—particularly for metal ions (*e.g.*, Au, Ag, Cu, Pd, Pt) that readily form complexes with primary amine ligands. However, the size of the resultant nanostructure is relatively large, with a greater degree of agglomeration possible.[25] This is especially the case for hyperbranched polymers that exhibit a random structure, which results in much greater polydispersity.[26] On the other hand, if the primary surface amines are replaced with hydroxyl or quaternary ammonium[27] groups, the pre-reduced metal ions are forced further into the interior of the dendritic structure. As a caveat for Au nanocluster growth, the precursor salt $HAuCl_4$ may be preferentially reduced by the surface hydroxyls, precluding its intra-dendrimer complexation.[28]

It should be noted that surface complexation (inter-dendrimer stabilization) also yields nanoparticles/nanoclusters (*e.g.*, nanoparticulate gold, silver, platinum metals,[31] iron oxide,[32,33] tin (and aluminium) oxide,[34] and II–VI semiconductors (*e.g.*, CdS[35])). For these systems, it is thought that the dendrimers act as colloidal stabilizers much like linear polymers or surfactants—resulting in much less control over resultant nanocluster sizes/properties. Similar complexation effects also result from varying the solution pH,[36] which affects the protonation of surface and interior amine groups, with pK_a

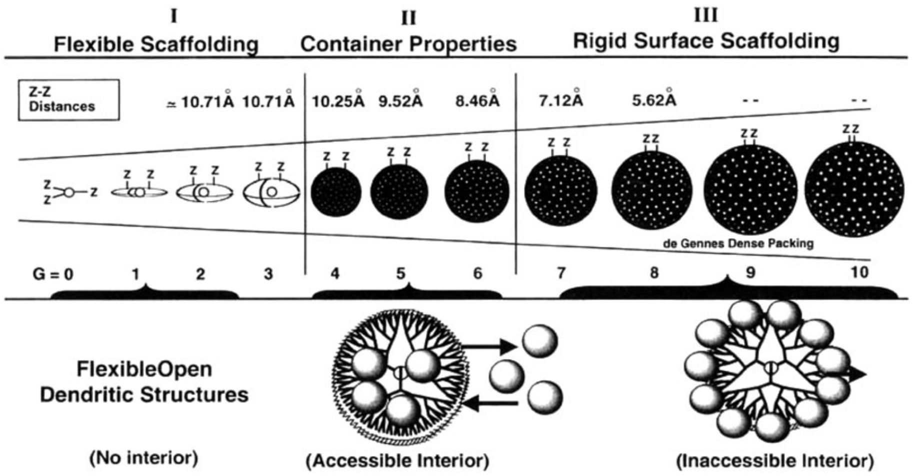

Fig. 2 Relative sizes and surface densities of PAMAM dendrimers, showing the most suitable range for nanoparticle growth as generation 4 to generation 6.[30]

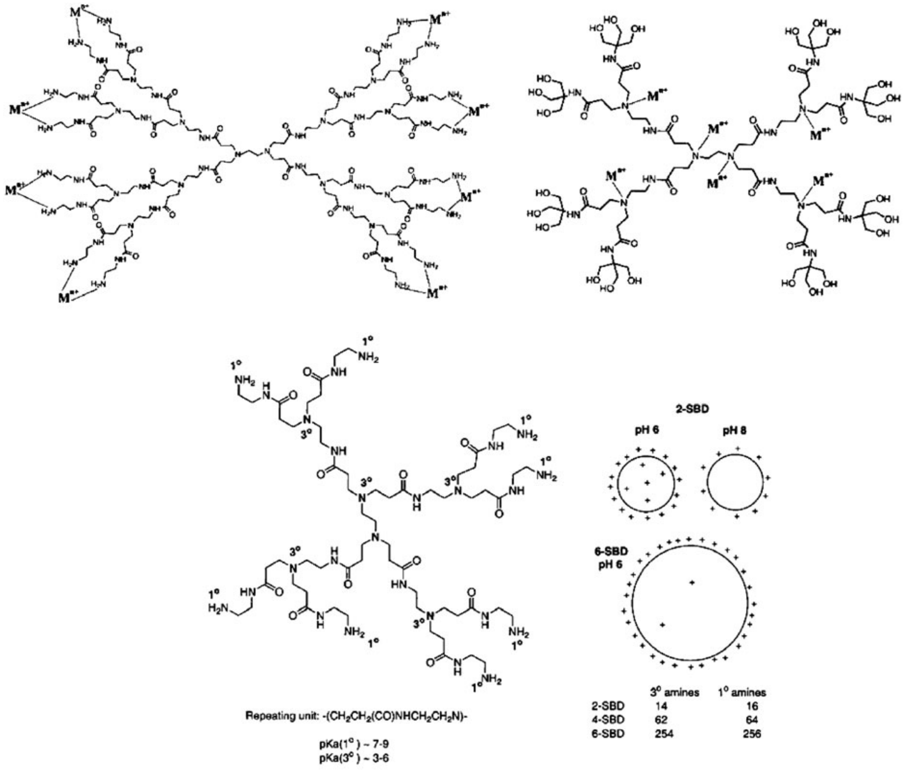

Fig. 3 Molecular structure of a second-generation (G2) amine-terminated PAMAM dendrimer, illustrating the positions of the metal ions chelated to the primary amine groups (pre-reduction). In comparison, a G2 hydroxyl-terminated PAMAM dendrimer is shown, with the metal ions now preferring to chelate to the interior tertiary amine groups. Shown on the bottom is the effect of protonation on G2/G6 amine-terminated PAMAM dendrimers. A schematic on the lower right illustrates the positions of the protonated amines at varying pH values. As the generation size increases, the surface density also increases which prevents the access of protons (or chelating metal ions) to interact with the interior tertiary amine groups.[39]

values of 7–9 and 3–6, respectively (Fig. 3).[37] At a pH of 2, the exterior primary amine groups are preferentially protonated relative to the interior tertiary amines.[38] Metal ions thereby compete with protons for amine chelation to the interior of the dendritic structure within highly acidic solutions. Hence, fine-tuning the solution pH for dendrimers containing primary and tertiary amine groups may afford either intra-dendrimer encapsulation, or inter-dendrimer stabilization, with the former resulting in much smaller diameters and extremely narrow polydispersities for the reduced metal nanoclusters.

As a further illustration of the extreme flexibility of the dendritic architecture, the core may also be altered to change its solubility characteristics, or allow a conduit for the penetration of species through the periphery at high generations (Fig. 4). Since dendrimers containing an almost unlimited range of cores and peripheral groups may be synthesized, it is now possible to easily control nanocluster properties such as composition, size, morphology, solubility and degree of encapsulation. One application of this latter property is to control the release rate of entrained medicinal agents/sensors based on structural or environmental changes, for targeted drug delivery or *in situ* monitoring.

As we have noted thus far, metal nanocluster growth using dendritic templates is strongly governed by the preferred complexation of the precursor metal ions with either primary or tertiary amine groups. Though Cu^{2+} has a strong affinity for both types of amines, Ag^+ is not strongly bound to tertiary amine groups. Hence, Ag nanoclusters are not possible using the standard complexation/chemical reduction route. However, a clever redox-facilitated route may be used, wherein Cu^0 nanoclusters are first generated within a hydroxyl-terminated dendrimer, followed by Ag^+ ion exposure. This will displace Cu^0 with Ag^0 within the dendrimer interior due to favorable redox potentials between these coinage metals (eqn (2)).[41]

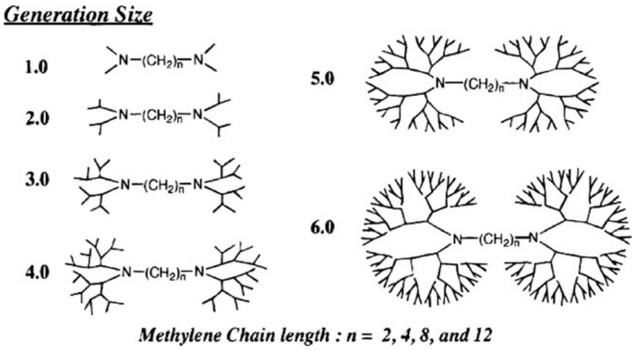

Fig. 4 Molecular structures of dendrimers modified with long-chain aliphatic cores. Unlike traditional dendritic structures with smaller cores, as the generation size increases, there is an available channel for external species to enter the dendrimer interior.[40]

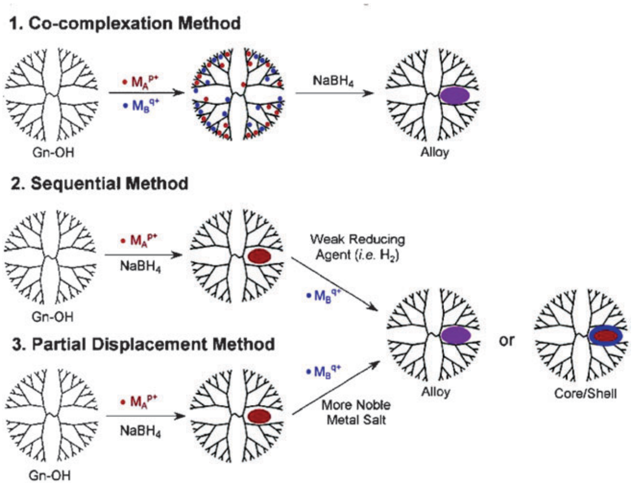

Fig. 5 Schematic of the three methods used to generate bimetallic nanoparticles within a dendritic host.[49]

$$\mathrm{Cu} + 2\,\mathrm{Ag}^{+} \rightarrow \mathrm{Cu}^{2+} + 2\,\mathrm{Ag} \qquad (2)$$

In addition to isolated metal nanoclusters, complex intermetallic species have also been synthesized through the introduction of more than one metal to the dendritic structure. There are three primary routes for the solution-phase synthesis of bimetallic nanoclusters within a dendrimer (Fig. 5).[42,43] In addition to being proven for core–shell nanoclusters,[44] these methods should also be amenable for the synthesis of trimetallic nanoclusters[45] for interesting catalytic applications.

In order to generate core–shell nanostructures, the core nanocluster is first formed *via* simple complexation/reduction. The shell is deposited selectively over the core nanocluster by using a weak reducing agent such as ascorbic acid (Fig. 6),[46] an excess of which also prevents premature reduction of Au^{3+} by the terminal –OH groups. The core–shell architecture was confirmed by evaluating its localized surface plasmon resonance (LSPR) profile, relative to encapsulated bimetallic co-complexation (alloy-like) nanostructures.

Thus far, we have discussed the synthesis of dendrimer-encapsulated nanoclusters within an aqueous medium, employing entraining agents with either terminal amine or hydroxyl groups. However, this limits the synthesis of metals (*e.g.*, Al, Ni, Fe, Co) that are easily oxidizable within such media. In order to phase-transfer dendrimer-stabilized nanoclusters into a nonpolar solvent, the aqueous nanocluster suspension is simply mixed with a nonaqueous phase containing alkylthiols.[47] Since the intra-dendrimer nanocluster is already formed prior to thiol functionalization, much smaller diameters and narrower polydispersity is achieved relative to early colloidal growth employing thiol-terminated surfactants, or recent precedents using long-chain hydrocarbon stabilizers.[48] As an alternative to phase-transfer additives, Crooks and co-workers have recently developed a strategy to prepare nanoclusters in a single step within organic solvents using hydrophobic-terminated dendrimers (Fig. 7).[50] This strategy has been applied to grow Au nanoparticles, with subsequent phase-transfer into aqueous solvents using water-soluble thiols (*e.g.*, tiopronin, glutathione).[44] More recently, zero-valent Ni nanoclusters with diameters <1.5 nm were synthesized using dodecyl-functionalized PAMAM dendrimers.[51] Though there is no precedent in the literature for zero-valent iron nanoclusters, this method should also be amenable for these structures.

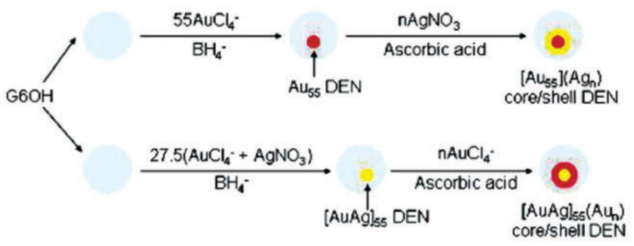

Fig. 6 The experimental conditions used to generate core–shell nanoclusters. Ascorbic acid is used as a weak reducing agent for shell deposition.[44]

The discovery of copoly(amidoamine-organosilicon) (PAMAMOS) dendrimers by Dvornic *et al.* in the late-1990s represented an important evolutionary step for hydrophobic-terminated entraining agents. This structure represents the first "copolymer dendrimer", which features both a hydrophilic PAMAM core and hydrophobic organosilicon shell (Fig. 8).[52] Due to the identical core structure as PAMAM, this class of dendrimers is able to encapsulate a number of metal ions and electrophilic organic/organometallic compounds.[53] Facile phase-transfer of these species into organic solvents is afforded through the organosilicon periphery, making this architecture extremely powerful for such syntheses.

Whereas (S)TEM/EDS[54,55] may be used to characterize the elemental composition of discrete nanoclusters in the 1–5 nm size regime, techniques such as UV-Vis[12,13] and EPR[56] spectroscopies are most commonly employed to describe the coordination environment of encapsulated metal ions.

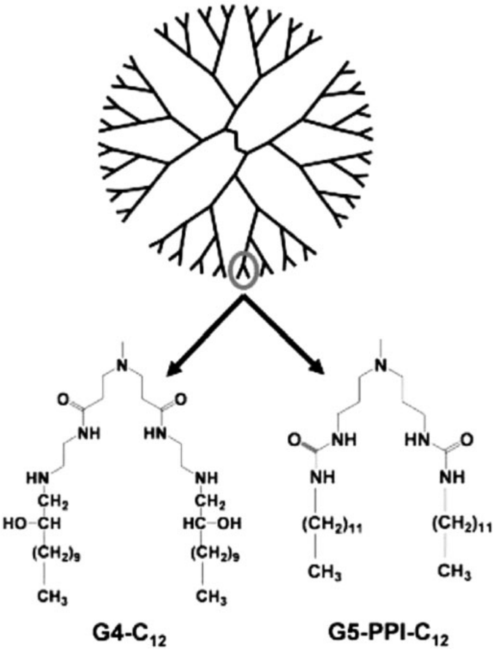

Fig. 7 Hydrophobic-functionalized PAMAM (G4-C_{12}) and poly(propyleneimine) (PPI) dendrimers, which served as templates for Au nanoparticle growth.[50]

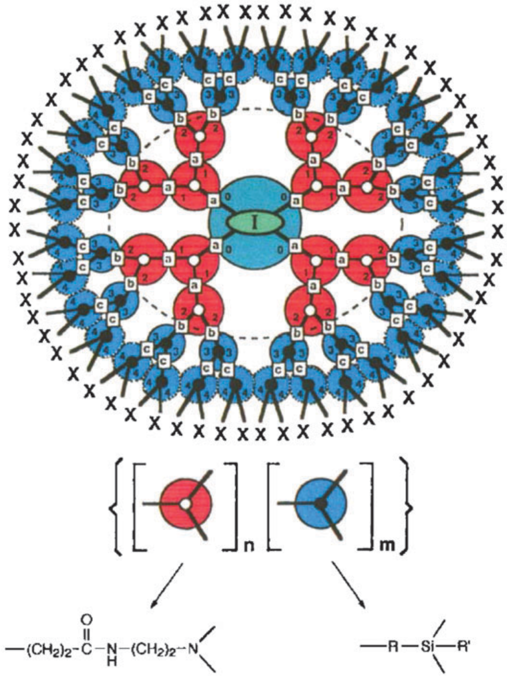

Fig. 8 Illustration of a poly(amidoamine-organosilicon), PAMAMOS, dendrimer, with two generations of each PAMAM and organosilicon units.[58]

However, a more detailed description was recently reported by Bubeck *et al.*, using near edge X-ray absorption fine structure (NEXAFS) of Cu^{2+}@PAMAMOS nanocomposites.[57] This study showed that the metal ions interact with both tertiary amine groups and oxygens from neighboring carbonyl groups. Interestingly, it was also shown that the interaction of the metal ion with the dendritic host was dependent on the counter anion present. For instance, counter Cl^- ions resulted in a two-fold reduction in Cu^{2+}/dendrimer complexation strength relative to SO_4^{2-} ions. This difference may be explained by considering the degree of interaction between the cation/anion pair. That is, during complexation of a metal salt with a dendrimer, it is possible that the counterions may exist as both free spectator anions and M^{n+}-coordinated ligands. As one would expect, only the latter interaction would have a detrimental influence on the M–N bonding. In particular, the *trans*-labilizing effect (*i.e.*, "*trans* effect") for substitution reactions involving square planar complexes (*e.g.*, Cu^{2+}, Pt^{2+}, *etc.*) is of similar magnitude for Cl^- and amines, which explains the significant decrease in Cu–N interaction in the presence of Cl^-. In contrast, complex anions such as sulfates and nitrates are more likely to exist as free ions due to their steric bulk.

3 Dendrimer-encapsulated nanoclusters: applications

3.1 Catalysis

The research arena has now progressed beyond the synthesis of nanoclusters, to now focusing on applications for these nanostructures. As one might expect, the primary application for metallic nanoclusters is homogeneous/heterogeneous catalysis. Crooks has previously distinguished the two by referring to DENs dissolved in solution as homogenous catalysts, and those attached to a support as heterogeneous; we shall use the same convention here.[59] The literature abounds with reports of DENs being used to catalyze hydrogenation, alcohol reduction, electrocatalytic O_2 reduction, and Suzuki, Stille, and Mizoroki–Heck coupling reactions;[60] we shall not attempt to describe each, but a few points and generalizations are noteworthy.

The dendritic architecture is especially suited for these applications, since the nanoclusters are extremely small (<5 nm) resulting in extraordinary available surface area, while being completely encapsulated, precluding surface saturation through inter-dendrimer interactions. In addition, the periphery may be fine-tuned to selectively allow the reactive species to approach the encapsulated nanosized catalyst. Also, since the surface of the dendrimer may be modified with a host of different groups, the solubility of the dendrimer can be altered for different solvents. The structural and compositional tunability of the dendritic architecture allows the opportunity for DENs to not only be selective toward different reactants, but products as well.[61]

With regards to reactant selectivity, in Pd DEN hydrogenation reactions, the density of the peripheral groups on the dendrimer surface and the size of the substrate were shown to be determining factors in the turnover frequency (TOF).[62] In particular, it was reported that greater steric crowding on the dendrimer surface resulted in a lower TOF for the substrate. Although it is rather intuitive that larger substrates would have more difficulty penetrating through a higher generation dendrimer's dense periphery than a smaller substrate penetrating a lower generation dendrimer's surface, size is not the only factor. Ooe *et al.* have discussed that more polar substrates experience a higher selectivity with Pd DENs than less polar substrates; furthermore, they attribute this to the interactions of polar substrates with interior amine groups of the dendrimer that enhance solubility and thus TOF.[63]

Heterogeneous catalysis utilizing DENs involves immobilizing them on some kind of solid support such as gold,[64] silica,[65] and titania[66] surfaces (*e.g.*, Fig. 9), or a polymer matrix.[67] The principal advantage of using dendrimers for this application is that nanoparticles can be synthesized and dispersed with minimal post-aggregation. Furthermore, this same methodology can be employed to produce layer-by-layer (LbL) thin film growth (*vida infra*). Due to the tunable periphery exhibited by dendritic entraining agents, the resultant nanocomposites are able to interact with a variety of surfaces. Most frequently, surface chemisorption is accomplished through the strong interaction of many surfaces with pendant $-NH_2$ and –OH groups, as featured in commercially-available PAMAM and PPI structures. As such, these dendritic classes are amenable for homogeneous film coverage using simple spin-coating techniques, with self-assembly of the encapsulated species on the substrate surface. For more homogeneous thin film deposition of encapsulated nanoclusters, Roberts and co-workers recently reported a pressure-tunable method employing the rapid expansion of supercritical CO_2 (RESS).[68] Following deposition, the dendrimer backbone may be removed through

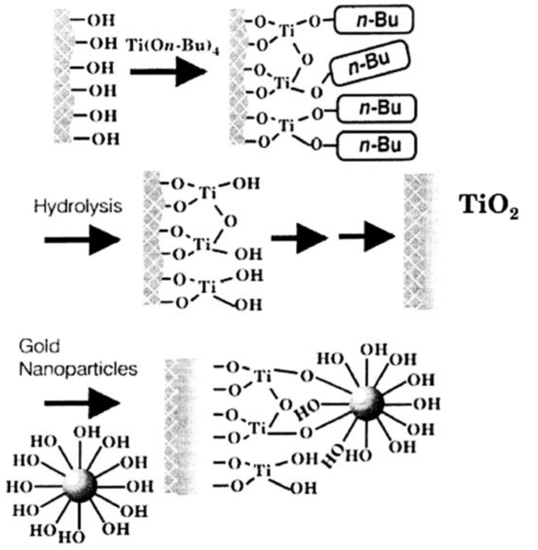

Fig. 9 Illustration of the chemisorption of a nanostructure onto a hydroxylated TiO_2 surface.[66] The hydroxyl groups on the periphery of the nanostructure stabilizing agent provide the handle for surface adsorption.

thermal annealing to afford template alignment of the nanoclusters.

3.2 Films/coatings

Polyelectrolyte-facilitated layer-by-layer (LbL) thin film growth remains an exciting area of investigation for the design of multifunctional coatings on a variety of substrates.[69] The earliest precedent for PAMAM film growth featured the alternating deposition of PAMAM dendrimers with positively charged peripheral amines and negatively charged carboxylic acid groups.[70] However, the first report of dendrimer-encapsulated nanocluster multilayer films was reported by Tomalia and co-workers using alternating layers of poly(sodium-4-styrenesulfonate) and Au@PAMAM nanoclusters.[71] As a nice combination of these earlier precedents, bimetallic multilayer films consisting of alternating layers of positively-charged Au@PAMAM (pH 3) and negatively-charged Ag@PAMAM (pH 11) was recently reported.[72] As one might expect, it is also possible to synthesize metallic nanostructures onto the surface of a pre-formed multilayer PAMAM film. This strategy has recently been demonstrated for the electrodeposition of Au/Pt bimetallic ''nanoflowers'' on a PAMAM-functionalized ITO substrate.[73] Through varying the electrodeposition conditions one is also able to change the morphology of the surface nanostructures, which is of extreme importance for catalytic applications.

The PAMAMOS dendrimer is ideally designed to interact with glass surfaces that contain reactive silanol (Si–OH) groups. As such, a permanent coating of the M@dendrimer nanocomposite may be realized, with a tunable surface adsorption based on the nature of the peripheral groups. Analogous to PAMAM, secondary interactions between the protonated tertiary amines and negatively-charged surfaces are also possible for these structures. Due to water-sensitive alkoxysilyl groups (*e.g.*, Si–OCH_3), facile PAMAMOS network formation may also be afforded, analogous to sol–gel formation of SiO_2 networks (Fig. 10).[74] The resultant nanostructured network, or surface-bound coatings (if desired) may prove instrumental for low-*k* interconnect coatings for next-generation CMOS ICs, of which there is a dire need for improvement. If nanoclusters are encapsulated within the PAMAMOS architecture prior to network formation, a homogeneous dispersion will result which may be of interest in the design of advanced materials such as selective-site catalysts, sensors, magnetic or conductive thin films, optoelectronic coatings, nanolithography,[75] and smart fabrics.

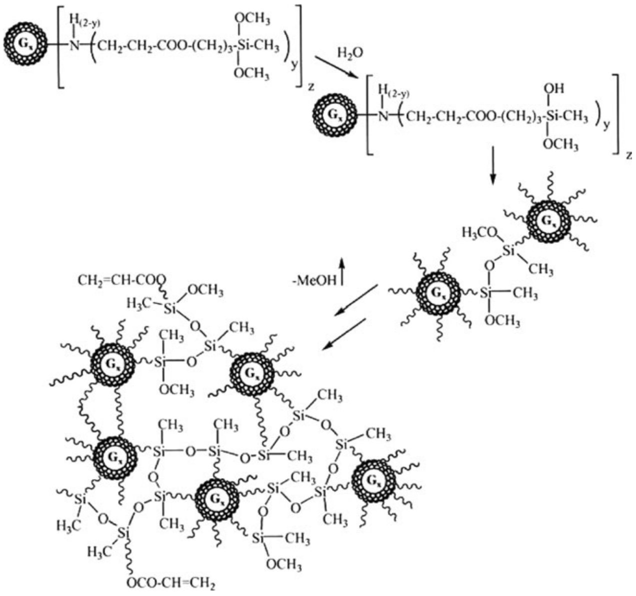

Fig. 10 Network (megamer) formation through the hydrolysis/cross-linking of neighboring PAMAMOS dendrimer units.[52b]

3.3 Carbon nanotubes

A recent application for dendrimer-encapsulated nanoclusters is for the controlled growth of carbon nanotubes (CNTs). These 1-D nanostructures have fascinated the scientific world since their discovery by Iijima in 1991.[76] Among the many methods used to synthesize CNTs, catalyzed chemical vapor deposition (CVD) represents the current method of choice. Although the exact mechanism involved in nanotubes growth is not completely understood, it has been demonstrated that the diameters of catalytically grown CNTs may be altered through changing the diameter and/or nature of the catalytic sites.[77] Dai and co-workers utilized dendrimers as carriers for the delivery of catalytic iron species onto a substrate surface (Fig. 11).[78] Following pyrolysis of the polymeric matrix, uniformly arranged iron oxide nanoparticles having a narrow size distribution (1–2 nm) allowed for the subsequent synthesis of single-walled nanotubes (SWNTs) with a narrow diameter distribution.

As an extension to this work, we have also investigated CNT growth utilizing a dendritic-based catalyst; however, we are evaluating a number of low-temperature routes in order to maintain the integrity of the CNT-dendrimer linkage. In addition to offering a novel nanoarchitecture for future

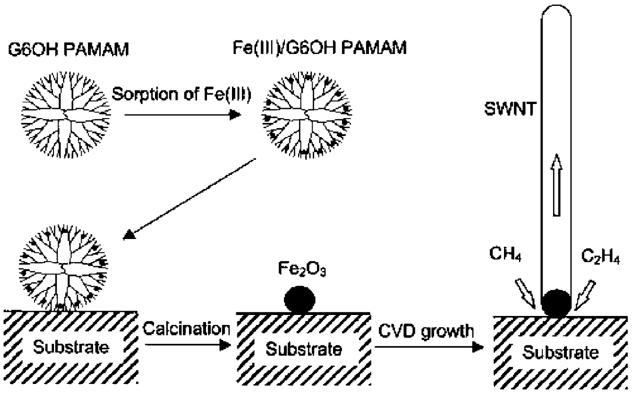

Fig. 11 A schematic showing the catalyzed growth of a carbon nanotube from a Fe_2O_3 nanoparticle derived from a PAMAM dendrimer template.

applications, such a linkage could potentially allow CNTs to be solubilized in organic solvents without having to actually chemically modify the surface of the CNTs.[79] Using a catalyst comprised of an amine-terminated G4 PPI dendrimer with stabilized iron oxide nanoparticles, we were able to grow multi-walled CNTs (MWNTs) at the lowest temperature to date (175 °C).[80] The growth occurred within supercritical CO_2, using CCl_4 as the carbon precursor. Due to inter-dendrimer stabilization through terminal primary amine groups, extensive catalyst agglomeration ensued, with resultant nanotubes exhibiting diameters of *ca.* 20–25 nm.

As an extension of this work towards milder synthetic conditions, we used the same catalyst at ambient temperature/pressure in the presence of tetrachloroethylene and potassium metal.[81] Surprisingly, a high yield (50%) of carbon nanofibers was generated, with aspect ratios of *ca.* 5000—much greater than other low-temperature precedents.[82,83] Although these nanofibers are poorly graphitized carbon and not graphitic nanotubes at room temperature, it is significant that this level of nanostructural carbon growth involved only solvent-mediated stirring on a benchtop.

Another recent use of this catalyst was reported for the growth of single-walled nanotubes (SWNTs) by plasma-enhanced CVD on a variety of substrates such as SiO_2/Si, Ti/Si, sapphire, and porous anodic alumina.[84] This work illustrated the problems associated with catalyst agglomeration through calcination of the dendritic host prior to CNT growth. Any increase in the polydispersity/size of the catalytic nanocluster will detract from the yield and purity of SWNTs, preferentially forming MWNTs and amorphous carbon structures.

3.4 Quantum dots

Dendrimer-entrained metallic nanoclusters have also been exploited in recent years for quantum dot applications.[85] Though quantum dots are typically thought of as semiconductor nanocrystals,[86] the electronic structure of a metal nanocluster is also critically dependent on its size. Though the size-tunable color of metallic nanoclusters is thought to arise solely from surface plasmon resonance effects, this phenomenon becomes significantly reduced for very small nanoclusters (*i.e.*, diameters *ca.* <3 nm). Instead, the continuous bands of energy levels become subdivided into discrete levels due to quantum confinement. Since there are relatively few atoms present in nanoclusters of this size regime, the spacings between adjacent energy levels (known as the Kubo gap, δ, will become comparable to the thermal energy, kT; especially at lower temperatures and smaller nanocluster sizes (eqn (3); E_f = Fermi level of the bulk metal, N = nuclearity of the nanocluster).[87]

$$\delta = 4E_f/3N \qquad (3)$$

This increasing bandgap for smaller diameters results in an observable blue emission, as well as a transition from metallic to insulating conductive properties (Fig. 12).[46]

Through use of dendritic stabilizers, one is now able to grow the smallest of metal nanoclusters, well within the range where quantum confinement occurs. For instance, dendrimer-encapsulated Au_8 nanoclusters were recently synthesized, emitting light in the blue spectral region with a quantum yield of 41%.[88] The high level of intra-dendritic stabilization was thought to facilitate the pronounced quantum efficiency (*ca.* two orders of magnitude larger than other Au nanoclusters), through isolation of the nanoclusters from quenchers in solution. However, this report is not without controversy; strong blue photoluminescence also results from hydroxyl-terminated PAMAM dendrimers in the absence of gold nanoparticles.[89] The simple oxidation of G0–G4 PAMAM with ammonium persulfate or ammonium hexafluorophosphate gave rise to a strong blue emission with a quantum yield approaching 60%. Interestingly, analogous experiments with amine-terminated PAMAM hosts did not give rise to photoluminescence, illustrating the importance of the peripheral groups on its photoactivity.

3.5 Biomedical applications

Dendrimers are currently being investigated for a number of biomedical applications,[90] most notably drug delivery[91] and

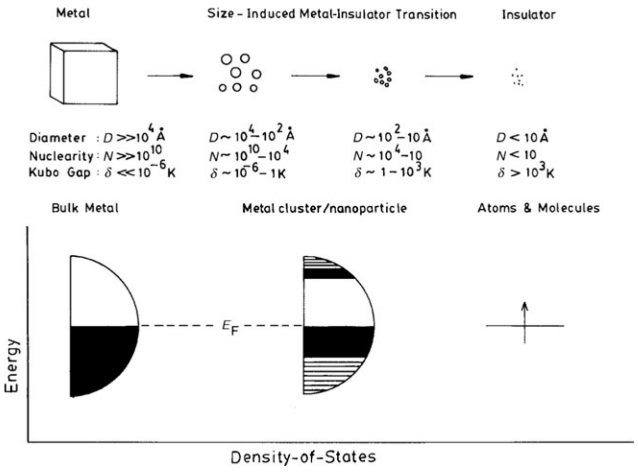

Fig. 12 Schematic of the energy levels exhibited by bulk metal relative to increasingly smaller nanoclusters. The approximate diameter, nuclearity, and Kubo gap for each size regime are indicated. In general, as the nanocluster size decreases, the electronic continuum exhibited by the bulk is transformed into discrete energy levels, especially at band edges.[87]

gene transfection.[92] However, most germane to the discussion of DENs is the application as antimicrobial and imaging agents. PAMAM dendrimer-based silver complexes and nanocomposites have been reported to be effective antimicrobial agents *in vitro* against *Staphylococcus aureus*, *Pseudomonas aeruginosa*, and *Escherichia coli*.[93] Furthermore, since PAMAM dendrimers are biocompatible,[94] it is possible to use these nanostructures as *in vivo* diagnostic fluorescent markers—most likely in combination with drug targeting/delivery dendrons, as recently reported by Baker and co-workers.[95] Specifically regarding imaging applications, dendrimers containing chelated Gd^{3+} have been used in MRI studies and dendrimer nanocomposites with gold and silver have shown promise as cell biomarkers. Balogh and co-workers have reported silver[96] and gold[97] dendrimer nanocomposites that are non-toxic, fluorescent, water soluble, and stable at biologic pH levels. Furthermore, *in vitro* labeling in normal and cancer cells showed a dependence of cellular uptake on surface charge with the positively charged species internalized most compared to neutral or positively charged species. Characteristics such as size, surface charge, and toxicity are tunable functions of the surface of the dendrimer templates.

Perspectives

The use of a dendritic host has greatly reduced the synthetic complexities associated with the growth of monodisperse nanoclusters. Though the synthesis of dendrimer-encapsulated metallic nanoarchitectures is becoming a mature field, there is ample room for growth in the synthesis of dendrimer-stabilized compound nanoclusters (oxides, sulfides, nitrides, phosphides, *etc*., and mixed phases thereof). Since *ca*. 2002 onwards, the field of nanotechnology has shifted from nanoarchitecture synthesis to a greater focus on applications. The field of dendrimer-encapsulated nanoclusters is no different; these exciting nanostructures will continue to find intriguing uses as we strive to supply worldwide needs related to alternative energy sources, remediation strategies for environmental pollution, faster/smaller electronic devices, homeland security (active sensors and self-decontaminating materials), "smart" materials, and many others.

In particular, two broad areas that will continue to increase the exploitation of dendritic-encapsulated nanoclusters are homeland security and medical fields. The ability to fine-tune the peripheral structure of the dendritic host is essential in the design of sensors that may detect chemical/biological warfare agents (in air, water or food sources), as well as toxins or viruses in the human body. However, what makes these architectures so unique is the ability to incorporate additional functionalities that will then respond to these external stimuli in an appropriate manner. For example, not only detecting and locating the presence of cancerous cells, but also delivering an anti-cancer drug directly to the infected cells. Though DEN synthesis is now a mature field, there is still a need for further structure/property investigations. For example, determining the degree of morphological/phase control that is possible within a dendritic architecture, and evaluating discrete influences of the dendritic host on the resultant properties of nanoclusters and coatings that comprise these species.

References

1 For instance, see: S. Stankic, M. Sterrer, P. Hofmann, J. Bernardi, O. Diwald and E. Knozinger, *Nano Lett*., 2005, **5**, 1889.
2 C.-C. Huang and H.-T. Chang, *Anal. Chem*., 2006, **78**, 8332.
3 For example, see: (*a*) N. N. Hoover, B. J. Auten and B. D. Chandler, *J. Phys. Chem. B*, 2006, **110**, 8606; (*b*) N. Zheng and G. D. Stucky, *J. Am. Chem. Soc*., 2006, **128**, 14278.
4 (*a*) J. Prabhuram, T. S. Zhao, Z. K. Tang, R. Chen and Z. X. Liang, *J. Phys. Chem. B*, 2006, **110**, 5245; (*b*) S. Fiechter, I. Dorbandt, P. Bogdanoff, G. Zehl, H. Schulenburg and H. Tributsch, *J. Phys. Chem. B*, 2007, **111**, 477.
5 For example (anti-corrosion applications), see: M. L. Zheludkevich, D. G. Shchukin, K. A. Yasakau, H. Mohwald and M. G. S. Ferreira, *Chem. Mater*., 2007, **19**(3), 402–411.
6 (*a*) J.-S. Choi, Y.-W. Jun, S.-I. Yeon, H. C. Kim, J.-S. Shin and J. Cheon, *J. Am. Chem. Soc*., 2006, **128**, 15982; (*b*) S. Jin and K. Ye, *Biotechnol. Prog*., 2007, **23**(1), 32–41.
7 http://en.wikipedia.org/wiki/Colloidal_gold.
8 C. N. R. Rao, G. U. Kulkarni, P. J. Thomas and P. P. Edwards, *Chem. Soc. Rev*., 2000, **29**, 27.
9 For examples of photolytic routes toward metal nanocluster growth within a dendritic entraining agent, see: (*a*) K. Sandor, T. Janos, D. Gyorgy, D. Lajos and Z. Miklos, *J. Colloid Interface Sci*., 2000, **229**, 550; (*b*) K. Esumi, A. Suzuki, N. Aihara, K. Usui and K. Torigoe, *Langmuir*, 1998, **14**, 3157.
10 J. Turkevich, P. S. Stevenson and J. Hillier, *Discuss. Faraday Soc*., 1951, **11**, 58.
11 T. Yonezawa, S. Onoue and N. Kimizuka, *Langmuir*, 2000, **16**, 5218.
12 M. Brust, M. Walker, D. Bethell, D. J. Schiffrin and R. Whyman, *J. Chem. Soc., Chem. Commun*., 1994, 801.
13 (*a*) R. G. Finke, D. K. Lyon, K. Nomiya, S. Sur and N. Mizuno, *Inorg. Chem*., 1990, **29**, 1784; (*b*) J. D. Aiken, Y. Lin and R. G. Finke, *J. Mol. Catal. A: Chem*., 1996, **114**, 29.
14 For a detailed discussion of the mechanistic steps, see: C. Besson, E. E. Finney and R. G. Finke, *J. Am. Chem. Soc*., 2005, **127**, 8179, and references therein.
15 R. G. Finke, in *Transition Metal Nanoclusters in Metal Nanoparticles: Synthesis, Characterization, and Applications*, Marcel-Dekker, New York, 2002.
16 R. E. Schaak, A. K. Sra, B. M. Leonard, R. E. Cable, J. C. Bauer, Y.-F. Han, J. Means, W. Teizer, Y. Vasquez and E. S. Funck, *J. Am. Chem. Soc*., 2005, **127**, 3506.
17 M. Tsuji, N. Miyamae, S. Lim, K. Kimura, X. Zhang, S. Hikino and M. Nishio, *Cryst. Growth Des*., 2006, **6**, 1801.
18 M. Chen, L.-W. Wang, J.-T. Han, J.-Y. Zhang, Z.-Y. Li and D.-J. Qian, *J. Phys. Chem. B*, 2006, **110**, 11224, and references therein.
19 K. Ohno, K.-M. Koh, Y. Tsujii and T. Fukuda, *Macromolecules*, 2002, **35**, 8989.
20 B. D. Fahlman, *Materials Chemistry*, Springer, New York, in press.
21 M. Zhao, L. Sun and R. M. Crooks, *J. Am. Chem. Soc*., 1998, **120**, 4877–4878.
22 L. Balogh and D. A. Tomalia, *J. Am. Chem. Soc*., 1998, **120**, 7355–7356.
23 (*a*) Crooks *et al*., *Nano Lett*., 2001, **1**, 14; (*b*) For another early use of PPI as an entraining agent for Cu sequestering, see: P. N. Floriano, C. O. Noble, J. M. Schoonmaker, E. D. Poliakoff and R. L. McCarley, *J. Am. Chem. Soc*., 2001, **123**, 10545.
24 H. Lang, R. A. May, B. L. Iversen and B. D. Chandler, *J. Am. Chem. Soc*., 2003, **125**, 14832.
25 For example, see: (*a*) M. F. Ottaviani, F. Montalti, N. J. Turro and D. A. Tomalia, *J. Phys. Chem. B*, 1997, **101**, 158; (*b*) R. Velarde-Ortiz and G. Larsen, *Chem. Mater*., 2002, **14**, 858; (*c*) X. Sun, S. Dong and E. Wang, *Macromolecules*, 2004, **37**, 7105; (*d*) M. E. Garcia, L. A. Baker and R. M. Crooks, *Anal. Chem*., 1999, **71**, 256.
26 Though the size dispersion of resultant nanoclusters may be somewhat controlled using hyperbranched polymers with a lower polydispersity. For example, see: S. Mecking, R. Thomann, H. Frey and A. Sunder, *Macromolecules*, 2000, **33**, 3958.
27 Y.-G. Kim, S.-K. Oh and R. M. Crooks, *Chem. Mater*., 2004, **16**, 167.

28 K. Esumi, T. Hosoya, A. Suzuki and K. Torigoe, *Langmuir*, 2000, **16**, 2978.
29 Reproduced from: (*a*) A. W. Jensen, B. S. Maru, X. Zhang, D. K. Mohanty, B. D. Fahlman, D. R. Swanson and D. A. Tomalia, *Nano Lett.*, 2005, **5**, 1171. Copyright 2005 American Chemical Society; (*b*) R. Velarde-Ortiz and G. Larsen, *Chem. Mater.*, 2002, **14**, 858. Copyright 2002, American Chemical Society.
30 Reproduced from *Dendrimers and other Dendritic Polymers*, ed. J. M. J. Frechet, D. A. Tomalia, Wiley, New York, 2001. Copyright 2001, Wiley-VCH.
31 (*a*) K. Esumi, A. Suzuki, A. Yamahira and K. Torigoe, *Langmuir*, 2000, **16**, 2604; (*b*) K. Torigoe, A. Suzuki and K. Esumi, *J. Colloid Interface Sci.*, 2001, **241**, 346–356.
32 E. Strable, J. W. M. Bulte, B. Moskowitz, K. Vivekanandan, M. Allen and T. Douglas, *Chem. Mater.*, 2001, **13**, 2201.
33 B. L. Frankamp, A. K. Boal, M. T. Tuominen and V. M. Rotello, *J. Am. Chem. Soc.*, 2005, **127**, 9731.
34 V. Juttukonda, R. L. Paddock, J. E. Raymond, D. Denomme, A. E. Richardson, L. E. Slusher and B. D. Fahlman, *J. Am. Chem. Soc.*, 2006, **128**, 420.
35 (*a*) L. H. Hanus, K. Sooklal, C. J. Murphy and H. J. Ploehn, *Langmuir*, 2000, **16**, 2621; (*b*) K. Sooklal, L. H. Hanus, H. J. Ploehn and C. J. Murphy, *Adv. Mater.*, 1998, **10**, 1083–1097; (*c*) J. R. Lackowics, I. Gryczynski, Z. Gryczynski and C. J. Murphy, *J. Phys. Chem. B*, 1999, **103**, 7613; (*d*) J. Huang, K. Sooklal, C. J. Murphy and H. J. Ploehn, *Chem. Mater.*, 1999, **11**, 3595.
36 J. Zheng, M. S. Stevenson, R. S. Hikida and P. G. Van Patten, *J. Phys. Chem. B*, 2002, **106**, 1252.
37 (*a*) M. S. Diallo, L. Balogh, A. Shafagati, J. H. Johnson, W. A. Goddard and D. A. Tomalia, *Environ. Sci. Technol.*, 1999, **33**, 820; (*b*) M. H. Kleinman, J. H. Flory, D. A. Tomalia and N. J. Turro, *J. Phys. Chem. B*, 2000, **104**, 11472.
38 (*a*) D. A. Tomalia, A. M. Naylor and W. A. Goddard, *Angew. Chem., Int. Ed. Engl.*, 1990, **29**, 138; (*b*) Y. Niu, L. Sun and R. M. Crooks, *Macromolecules*, 2003, **36**, 5725.
39 Reproduced from M. H. Kleinman, J. H. Flory, D. A. Tomalia and N. J. Turro, *J. Phys. Chem. B*, 2000, **104**, 11472. Copyright 2000, American Chemical Society.
40 Reproduced from D. M. Watkins, Y. Sayed-Sweet, J. W. Klimash, N. J. Turro and D. A. Tomalia, *Langmuir*, 1997, **13**, 3136. Copyright 1997, American Chemical Society.
41 M. Zhao and R. M. Crooks, *Chem. Mater.*, 1999, **11**, 3379.
42 R. M. Crooks, M. Zhao, L. Sun, V. Chechik and L. K. Yeung, *Acc. Chem. Res.*, 2001, **34**, 181, and references therein.
43 (*a*) R. W. J. Scott, A. K. Datye and R. M. Crooks, *Catal. Lett.*, 2003, **125**, 3708; (*b*) Y. M. Chung and H. K. Rhee, *Catal. Lett.*, 2003, **85**, 159; (*c*) Y.-M. Chung and H.-K. Rhee, *J. Mol. Catal. A: Chem.*, 2003, **206**, 291.
44 O. M. Wilson, R. W. J. Scott, J. C. Garcia-Martinez and R. M. Crooks, *J. Am. Chem. Soc.*, 2005, **127**, 1015.
45 For an example of trimetallic nanoparticle synthesis (using a non-dendritic host), see: A. Henglein, *J. Phys. Chem. B*, 2000, **104**, 6683.
46 R. W. J. Scott, O. M. Wilson, S.-K. Oh, E. A. Kenik and R. M. Crooks, *J. Am. Chem. Soc.*, 2004, **126**, 15583.
47 (*a*) J. C. Garcia-Martinez and R. M. Crooks, *J. Am. Chem. Soc.*, 2004, **126**, 16170–16178; (*b*) J. C. Garcia-Martinez, R. W. J. Scott and R. M. Crooks, *J. Am. Chem. Soc.*, 2003, **125**, 11190–11191; (*c*) Y.-G. Kim, J. C. Garcia-Martinez and R. M. Crooks, *Langmuir*, 2005, **21**, 5485–5491.
48 For example, see: S. Sun and H. Zeng, *J. Am. Chem. Soc.*, 2002, **124**, 8204.
49 Reproduced from R. W. J. Scott, O. M. Wilson and R. M. Crooks, *J. Phys. Chem. B*, 2004, **109**, 692. Copyright 2004, American Chemical Society.
50 M. R. Knecht, J. C. Garcia-Martinez and R. M. Crooks, *Langmuir*, 2005, **21**, 11981.
51 M. R. Knecht, J. C. Garcia-Martinez and R. M. Crooks, *Chem.-Mater.*, 2006, **18**, 5039.
52 (*a*) P. R. Dvornic, A. M. de Leuze-Jallouli, M. J. Owen and S. V. Perz, *Macromolecules*, 2000, **33**, 5366; (*b*) P. R. Dvornic, J. Li, A. M. de Leuze-Jallouli, S. D. Reeves and M. J. Owen, *Macromolecules*, 2002, **35**, 9323.
53 P. R. Dvornic, *J. Polym. Sci., Part A: Polym. Chem.*, 2006, **44**, 2755, and references therein.
54 For example, see: R. W. J. Scott, C. Sivadinarayana, O. M. Wilson, Z. Yan, D. W. Goodman and R. M. Crooks, *J. Am. Chem. Soc.*, 2005, **127**, 1380.
55 (*a*) I. Arslan, T. J. V. Yates, N. D. Browning and P. A. Midgley, *Science*, 2005, **309**, 2195; (*b*) M. F. Chisholm, S. Kumar and P. Hazzledine, *Science*, 2005, **307**, 701.
56 M. F. Ottaviani, R. Valluzzi and L. Balogh, *Macromolecules*, 2002, **35**, 5105.
57 R. A. Bubeck, P. R. Dvornic, J. Hu, A. Hexemer, X. Li, S. E. Keinath and D. A. Fischer, *Macromol. Chem. Phys.*, 2005, **206**, 1146.
58 Reproduced from P. R. Dvornic and M. J. Owen, in *Synthesis and Properties of Silicones and Silicone-Modified Materials*, ACS Symposium Series 838, Washington, DC, 2002, p. 236.
59 R. W. J. Scott, O. M. Wilson and R. M. Crooks, *J. Phys. Chem. B*, 2005, **109**, 692–704.
60 For instance: (*a*) for a thorough recent review of catalytic applications for DENs, see: R. W. J. Scott, O. M. Wilson and R. M. Crooks, *J. Phys. Chem. B*, 2005, **109**, 692; (*b*) R. W. J. Scott, A. K. Datye and R. M. Crooks, *J. Am. Chem. Soc.*, 2003, **125**, 3708–3709; (*c*) M. Zhao and R. M. Crooks, *Angew. Chem., Int. Ed.*, 1999, **38**, 364–366; (*d*) M. Zhao and R. M. Crooks, *Adv. Mater.*, 1999, **11**, 217–220; (*e*) H. Ye and R. M. Crooks, *J. Am. Chem. Soc.*, 2005, **127**, 4930–4934; (*f*) L. K. Yeung and R. M. Crooks, *Nano Lett.*, 2001, **1**, 14–17; (*g*) E. H. Rahim, F. S. Kamounah, J. Frederiksen and J. B. Christensen, *Nano Lett.*, 2001, **1**, 499–501; (*h*) R. Narayanan and M. A. El-Sayed, *J. Phys. Chem. B*, 2004, **108**, 8572–8580; (*i*) J. C. Garcia-Martinez, R. Lezutekong and R. M. Crooks, *J. Am. Chem. Soc.*, 2005, **127**, 5097–5103; (*j*) K. Esumi, R. Isono and T. Yoshimura, *Langmuir*, 2004, **20**, 237; (*k*) O. M. Wilson, M. R. Knecht, J. C. Garcia-Martinez and R. M. Crooks, *J. Am. Chem. Soc.*, 2006, **128**, 4510; (*l*) N. N. Hoover, B. J. Auten and B. D. Chandler, *J. Phys. Chem. B*, 2006, **110**, 8606.
61 L. K. Yeung, C. T. Lee, K. P. Johnston and R. M. Crooks, *Chem. Commun.*, 2001, 2290–2291.
62 For instance, see: (*a*) S.-K. Oh, Y. Niu and R. M. Crooks, *Langmuir*, 2005, **21**, 10209; (*b*) Y. Niu, L. K. Yeung and R. M. Crooks, *J. Am. Chem. Soc.*, 2001, **123**, 6840–6846.
63 M. Ooe, M. Murata, T. Mizugaki, K. Ebitani and K. Kaneda, *Nano Lett.*, 2002, **2**, 999–1002.
64 H. Ye, R. W. J. Scott and R. M. Crooks, *Langmuir*, 2004, **20**, 2915–2920.
65 H. Lang, R. A. May, B. L. Iversen and B. D. Chandler, *J. Am. Chem. Soc.*, 2003, **125**, 14832–14836.
66 S. Liu, T. Zhu, R. Hu and Z. Liu, *Phys. Chem. Chem. Phys.*, 2002, **4**, 6059.
67 J. Alvarez, L. Sun and R. M. Crooks, *Chem. Mater.*, 2002, **14**, 3995–4001.
68 J. Liu, M. Anand and C. B. Roberts, *Langmuir*, 2006, **22**, 3964.
69 For a nice review article on LbL, see: Paula Hammond's review article: P. T. Hammond, Form and function in multilayer assembly: New applications at the nanoscale, *Adv. Mater.*, 2004, **16**, 1271–1293.
70 V. V. Tsukruk, F. Rinderspacher and V. N. Bliznyuk, *Langmuir*, 1997, **13**, 2171.
71 J.-A. He, R. Valluzzi, K. Yang, T. Dolikhanyan, C. Sung, J. Kumar, S. K. Tripathy, L. Samuelson, L. Balogh and D. A. Tomalia, *Chem. Mater.*, 1999, **11**, 3268.
72 K. Esumi, S. Akiyama and T. Yoshimura, *Langmuir*, 2003, **19**, 7679.
73 L. Qian and X. Yang, *J. Phys. Chem. B*, 2006, **110**, 16672.
74 For example, see: P. R. Dvornic, R. A. Bubeck, S. D. Reeves, J. Li and L. W. Hoffman, *Silicon Chem.*, 2003, **2**, 207.
75 For example, see: N. Kohli, P. R. Dvornic, S. N. Kaganove, R. M. Worden and H. Lee, *Macromol. Rapid Commun.*, 2004, **25**, 935.
76 S. Iijima, *Nature*, 1991, **354**, 56.
77 C. L. Cheung, *J. Phys. Chem. B*, 2002, **106**, 2429.
78 (*a*) H. C. Choi, W. Kim, D. Wang and H. Dai, *J. Phys. Chem. B*, 2002, **106**, 12361. It should be noted that the first precedent for dendrimer-facilitated delivery of catalytic metals onto a substrate surface is reported in; (*b*) R. M. Crooks and M. Zhao, *Adv. Mater.*, 1999, **11**, 217.

79 For precedents related to surface-functionalization of CNTs with dendrimers, see: (*a*) S. Campidelli, C. Sooambar, E. L. Diz, C. Ehli, D. M. Guldi and M. Prato, *J. Am. Chem. Soc.*, 2006, **128**, 12544; (*b*) Y.-P. Sun, W. Huang, Y. Lin, K. Fu, A. Kitaygorodski, L. A. Riddle, Y. Joy Yu and D. L. Caroll, *Chem. Mater.*, 2001, **13**, 2864; (*c*) M. Holzinger, J. Abraham, P. Whelan, R. Graupner, L. Ley, F. Hennrich, M. Kappes and A. Hirsch, *J. Am. Chem. Soc.*, 2003, **125**, 8566.

80 J. K. Vohs, J. J. Brege, J. E. Raymond, A. E. Brown, G. L. Williams and B. D. Fahlman, *J. Am. Chem. Soc.*, 2004, **126**, 9936.

81 J. K. Vohs, J. E. Raymond, J. J. Brege and G. L. Williams, *Polym. News*, 2005, **30**, 330.

82 Y. Jiang, Y. Wu, S. Zhang, C. Xu, W. Yu, Y. Xie and Y. Qian, *J. Am. Chem. Soc.*, 2000, **122**, 12383.

83 X. Wang, J. Lu, Y. Xie, G. Du, Q. Guo and S. Zhang, *J. Phys. Chem. B*, 2002, **106**, 933.

84 P. B. Amama, M. R. Maschmann, T. S. Fisher and T. D. Sands, *J. Phys. Chem. B*, 2006, **110**, 10636.

85 For instance, see: (*a*) J. Zheng and R. M. Dickson, *J. Am. Chem. Soc.*, 2002, **124**, 13982; (*b*) K. Sooklal, L. H. Hanus, H. J. Ploehn and C. J. Murphy, *Adv. Mater.*, 1998, **10**, 1083.

86 For an example of intra-dendrimer stabilized CdS quantum dot nanoclusters, see: B. I. Lemon and R. M. Crooks, *J. Am. Chem. Soc.*, 2000, **122**, 12886.

87 C. N. R. Rao, G. U. Kulkarni, P. J. Thomas and P. P. Edwards, *Chem. Soc. Rev.*, 2000, **29**, 27.

88 J. Zheng, J. T. Petty and R. M. Dickson, *J. Am. Chem. Soc.*, 2003, **125**, 7780.

89 W. I. Lee, Y. Bae and A. J. Bard, *J. Am. Chem. Soc.*, 2004, **126**, 8358.

90 S. Svenson and D. A. Tomalia, *Adv. Drug Delivery Rev.*, 2005, **57**, 2106–2129.

91 For instance, see: (*a*) U. Boas and P. M. H. Heegaard, *Chem. Soc. Rev.*, 2004, **33**, 43–63; (*b*) J. M. J. Frechet, *Pharm. Sci. Technol. Today*, 2000, **2**, 393–401.

92 L. A. Kubasiak and D. A. Tomalia, Cationic Dendrimers as Gene Transfection Vectors, , in *Polymeric Gene Delivery: Principles and Applications*, ed. M. M. Amiji, CRC Press, Boca Raton, FL, 2004, pp. 133–157.

93 L. Balogh, D. R. Swanson, D. A. Tomalia, G. L. Hagnauer and A. T. McManus, *Nano Lett.*, 2001, **1**, 18–21.

94 (*a*) N. Belcheva, S. P. Baldwin and W. M. J. Saltzman, *Biomater. Sci. Polym. Ed.*, 1998, **9**, 207; (*b*) N. Belcheva, K. Woodrow-Mumford, M. J. Mahoney and W. M. Saltzman, *Bioconjugate Chem.*, 1999, **10**, 932.

95 I. J. Majoros, A. Myc, T. Thomas, C. Mehta and J. R. Baker, *Biomacromolecules*, 2006, **7**, 572.

96 W. Lesniak, A. U. Bielinska, K. Sun, K. W. Janczak, X. Shi, J. R. Baker and L. P. Balogh, *Nano Lett.*, 2005, **5**, 2123.

97 (*a*) A. Bielinska, J. D. Eichman, I. Lee, J. R. Baker and L. P. Balogh, *J. Nanopart. Res.*, 2002, **4**, 395; (*b*) X. Shi, T. R. Ganser, K. Sun, L. P. Balogh and J. R. Baker, *Nanotechnology*, 2006, **17**, 1072.